Journal of Physical Chemistry & Biophysics

You and Zhao, J Phys Chem Biophys 2016, 6:1
DOI: 10.4172/2161-0398.1000199

Research Article Open Access

Synthesis, Characterization and Visible Photocatalytic Performance of Iron (III) Tetracarboxyphthalocyanine-Sensitized TiO_2 Photocatalyst

Huimin You and Yanying Zhao*

Department of Chemistry, Zhejiang Sci-Tech University, Hangzhou 310018, PR China

Abstract

Fe (III) 2, 9, 16, 23-phthalocyanine tetracarboxylic acid [$FePc(COOH)_4$], synthesized via the reaction of trimellitic anhydride and urea at their melting points, was used to sensitize titanium dioxide by impregnation and adsorption. Ultraviolet-visible spectroscopy showed that the catalyst could effectively degrade photosensitive organic dyes, such as methylene blue, rhodamine B, neutral red, acid red, and malachite green. With an exposure time of 100 min, the degradation rate for all the dyes was >80%. In addition, in the case of rhodamine B, the $FePc(COOH)_4/TiO_2$ system showed the best degradation efficiency at pH=6. To investigate the relationship between degradation concentration and illumination time, first-order degradation kinetics equations were derived. Upon loading TiO_2 with phthalocyanine, the photoactivity of TiO_2 was extended to the visible light region, potentially enabling the use of solar energy for the photodegradation of organic dyes and other pollutants in wastewater.

Keywords: Iron phthalocyanine; TiO_2; Photocatalytic degradation; Organic dye; First-order reaction kinetics

Introduction

Nanometer-sized semiconductor photocatalysts use light to degrade organic matter in water and air. Because of its high photocatalytic activity, strong corrosion resistance, stability, and environmentally benign nature, TiO_2 has been widely studied for use in photocatalytic degradation [1-4]. However, TiO_2 has a wide bandgap (of about 3.2 eV) and can only absorb ultraviolet (UV) wavelengths <387 nm (only 4% of sunlight). However, TiO_2 can be modified to extend the light adsorption to the visible region. Doping with transition metals or non-metals [5,6], surface deposition of noble metals [7,8], and dye-sensitization [9] are some methods used to modify TiO_2. Among these methods, dye-sensitization of TiO_2, which involves the adsorption of a sensitizer dye on the TiO_2 surface, is a simple and effective strategy. The dye molecules upon exposure to visible light are excited, and the electrons are injected into the conduction band of TiO_2. These conduction band electrons react with oxygen adsorbed on the TiO_2 surface and form superoxide anion radicals (O_2^-), hydroxyl anion radicals, and other active species. These reactive species, in turn, can oxidize and degrade organic pollutants [10-12].

Among various sensitizers, phthalocyanine, an aromatic conjugated complex consisting of nitrogen and carbon atoms (eight each), is widely used. Phthalocyanine shows good absorption in the visible light region, and its molecular structure can be modified as desired. However, the applications of unsubstituted phthalocyanine are limited because of its insolubility in water and organic solvents. Sulfonic acid or carboxyl functional groups can be introduced into the benzene rings of the metal phthalocyanine to greatly improve their water solubility. What's more, phthalocyanine produces extremely reactive singlet oxygen ($^1O_2$) [13,14], which can render the photocatalytic process nonselective. Recently, metal phthalocyanine-sensitized titanium dioxides have been applied for the degradation of organic dyes and other pollutants in wastewater, because of their good photocatalytic performance [15-21].

In this study, 1, 2, 4-benzenetricarboxylic anhydride, urea, and a metal salt were used to synthesize iron phthalocyanine substituted with four carboxyl groups, by a solid catalytic method. Then, the substituted phthalocyanine ($FePc(COOH)_4$) was used to sensitize TiO_2 by dipping adsorption. The phthalocyanine and sensitized TiO_2 were characterized by ultraviolet (UV)-visible and fluorescence spectroscopy, nitrogen adsorption-desorption measurements, X-ray diffraction (XRD), Fourier transform infrared spectroscopy (FT-IR), and a series of other characterization techniques. The photocatalytic activity of the dye sensitized TiO_2 was analyzed by using it for the degradation of methylene blue (MB), rhodamine B (RB), acid red (AR), neutral red (NR), and malachite green (MG) under visible light radiation. We also investigated the influence of the pH of the solution on the degradation. Finally, we elucidated the photodegradation mechanism using photoluminescence (PL) and X-ray photoelectron spectroscopy (XPS).

Materials and Methods

Preparation of $FePc(COOH)_4$ and $FePc(COOH)_4/TiO_2$

The synthesis of Fe (III) 2, 9, 16, 23-phthalocyanine tetracarboxylic acid ($FePc(COOH)_4$).$FeCl_3 \cdot 6H_2O$, urea, and trimellitic anhydride (molar ratio=0.25:20:1) were used as the raw materials to prepare $FePc(COOH)_4$ by a solid fusion method, and the product was purified [22].

The catalyst was prepared by following the procedure described by Roman et al. [23] An aqueous suspension of TiO_2 (1 g/dm, 300 cm^3) was magnetically stirred for 10 min and ultrasonicated for 20 min. Then, $FePc(COOH)_4$ solution (10 cm^3, 5×10^{-3} mol/dm) in dimethyl sulfoxide (DMSO) was added to the TiO_2 aqueous suspension under stirring, and the solution was mixed overnight. The particles were collected by centrifugation; washed thoroughly with distilled water, ethanol, and acetone; and dried in a vacuum oven at 60°C. The resulting green powder was then ground in an agate mortar and stored in the dark.

***Corresponding author:** Yanying Zhao, Department of Chemistry, Zhejiang Sci-Tech University, Hangzhou 310018, PR China, Tel: +8657186843627; E-mail: yyzhao@zstu.edu.cn

Received November 24, 2015; **Accepted** January 03, 2016; **Published** January 06, 2016

Citation: You H, Zhao Y (2016) Synthesis, Characterization and Visible Photocatalytic Performance of Iron (III) Tetracarboxyphthalocyanine-Sensitized TiO_2 Photocatalyst. J Phys Chem Biophys 5: 199. doi:10.4172/2161-0398.1000199

Photocatalytic experiments

A halogen lamp (300 W) equipped with a cutoff filter at 400 nm was used as the irradiation source, and a Pyrex glass vessel (120 mL) was used as the reaction vessel. Before irradiation, the aqueous suspension (100 mL) containing 0.05 g of the catalyst and 100 mL of the organic substrate were stirred for 30 min. During the reaction, 2.0 mL of the suspension was withdrawn and separated by centrifugation. The absorbance at a specific wavelength was measured at 20 min intervals with a UV-visible spectrometer. $FePc(COOH)_4$ was dissolved in DMSO to record the UV-visible spectra. The analysis of the XPS binding energies were calibrated against the standard C 1s peak (at 285 eV).

Results and Discussion

Characterization of $FePc(COOH)_4$ and $FePc(COOH)_4/TiO_2$

The UV-visible spectrum of tetracarboxyphthalocyanine mainly originates from the $\pi \rightarrow \pi^*$ transitions of the strong Q-band (600-800 nm) and the broad B-band (300-450 nm). Quantum chemistry shows that the formation of the Q and B-bands are attributed to the $a_{1u}(\pi) \rightarrow e_g(\pi^*)$ and $a_{2u}(\pi) \rightarrow e_g(\pi^*)$ electronic transitions [24,25]. $FePc(COOH)_4$ exhibited strong Q-band and B-band adsorptions at λ_{max}=673 nm and 331 nm, respectively (Figure S1). The FT-IR spectra of TiO_2 (a), $FePc(COOH)_4$ (b), and $FePc(COOH)_4/TiO_2$ (c) samples are shown in Figure S2. The characteristic amide absorption peak occurs at around 1704 cm^{-1} (spectrum b) [26]. An absorption band at 400-800 cm^{-1} corresponds to the Ti-O bond stretching vibration (spectrum a) and the absorption bands at 1610 and 3000 cm^{-1} represent the vibrations of adsorbed water [27]. Because of the strong background absorption of TiO_2 and the small amount of $FePc(COOH)_4$, characteristic $FePc(COOH)_4$ absorption peaks were not observed in the FT-IR spectrum of the $FePc(COOH)_4/TiO_2$ sample at 400-800 cm^{-1}. However, characteristic amide absorption peaks at 1700 cm^{-1} were observed (spectrum c), indicating that the $FePc(COOH)_4$ molecules were adsorbed on the TiO_2 surface.

The N_2 adsorption-desorption isotherm and pore size distribution curve of $FePc(COOH)_4/TiO_2$ are shown in Figure S3. The Brunauer-Emmett-Teller (BET) surface areas and the mean pore size of the TiO_2 sample were 58.36 m^2/g and 10.0 nm, respectively. After sensitizing with $FePc(COOH)_4$, the BET surface area was 53.35 m^2/g and the pore size remained nearly unchanged. This demonstrates that $FePc(COOH)_4$ had combined with TiO_2 and occupied a certain fraction of the surface area. In addition, the large BET surface area could facilitate more efficient contact of TiO_2 with the organic dye, improving its photocatalytic activity.

The XRD patterns of the various samples are shown in Figure 1. $FePc(COOH)_4$, showed a broad weak peak at ~ 20° and a sharp strong peak at ~ 27° [28]. The XRD pattern of $FePc(COOH)_4/TiO_2$ is essentially identical to that of TiO_2. Therefore, the loading of the dye did not appear to change the crystalline structure or size of TiO_2. We assume that the dye molecules did not enter the crystal lattice and that the dye molecules and TiO_2 interact through van der Waals forces or hydrogen bonds.

The UV-visible diffuse reflectance spectra of the pure TiO_2 nanoparticles, $FePc(COOH)_4$, and $FePc(COOH)_4/TiO_2$ are shown in Figure 2. As observed in Figure 2 (spectrum a), the spectrum of the TiO_2 nanoparticles exhibited absorption only in the UV region and absorption was absent in the visible wavelengths. $FePc(COOH)_4/TiO_2$ exhibited absorption bands at 650-750 nm, which could be attributed to the Q-band of $FePc(COOH)_4$. Absorption bands at 650-750 nm were also observed in the spectrum of pure $FePc(COOH)_4$ (spectrum b, Figure 2). Hence, the sensitization of TiO_2 with $FePc(COOH)_4$ could extend the absorbance spectrum of TiO_2 into the visible region.

The photocatalysis efficiency is determined by the balance between the charge separation and recombination processes both in the bulk and on the surface. PL spectra, which directly arise from the radiative recombination processes of the electrons and holes of two different energy states, can be used to evaluate the charge recombination rate. Therefore, the PL spectra were obtained from TiO_2, $FePc(COOH)_4$, and $FePc(COOH)_4/TiO_2$ (Figure 3). The higher the PL emission intensity, the higher is the recombination rate of the photogenerated electrons and holes. The strength of the fluorescence intensity varies in the order TiO_2>$FePc(COOH)_4/TiO_2$>$FePc(COOH)_4$. This indicates that the energy transfer between TiO_2 and $FePc(COOH)_4$ reduces the fluorescence intensity, while improving the photocatalytic efficiency.

As seen in Figure 4, the full XPS scans (Figure 4A) demonstrate the presence of Ti, O, and C in pure TiO_2, while Ti, Fe, O, N, and C were present in $FePc(COOH)_4/TiO_2$. The presence of C in TiO_2 can be ascribed to adventitious carbon-based contaminants. The high-resolution XPS profiles corresponding to the Ti 2p region at around 460 eV, the Fe 2p region around 720 eV, and O1s region around 530 eV were analyzed. As shown in Figure 5B, two peaks were present in the Ti 2p region. The peak at 464.2 eV corresponds to the Ti $2p_{3/2}$. The difference in the Ti $2p_{1/2}$ and Ti $2p_{3/2}$ peak positions is 5.7 eV, indicating the presence of Ti^{4+} in the as-prepared $FePc(COOH)_4/TiO_2$ [29,30]. Further, the Ti 2p peaks of $FePc(COOH)_4/TiO_2$ showed no shift in comparison to the peak shown by pure TiO_2, confirming that the structure of TiO_2 remained intact after the synthesis of $FePc(COOH)_4/TiO_2$. In the Fe 2p region (Figures 4C and D), the peaks at 710.1 and 723.5 eV were attributed to Fe $2p_{3/2}$ and Fe $2p_{1/2}$, respectively, indicating the + 3 valency of Fe in $FePc(COOH)_4$. As seen in Figure 4E, the O 1s peak of $FePc(COOH)_4$ split into two peaks, with one centered at 531.2 eV (corresponding to the C-OH bond in the carboxyl group) and the second peak at 532.1 eV (corresponding to the C=O bond). After the sensitization of TiO_2 with $FePc(COOH)_4$, the O 1s binding energy was reduced from 531.2 eV to 529.9 eV (Figure 4F), demonstrating electronic coupling between $FePc(COOH)_4$ and TiO_2. This effect may be caused by the hydrogen bonds formed between the -COOH and -OH groups in $FePc(COOH)_4$ and on TiO_2 surface, respectively. The carboxyl group promotes the electronic coupling between the electron donating TiO_2 and electron accepting $FePc(COOH)_4$ [31]. The XPS signals of N 1s in $FePc(COOH)_4$ and $FePc(COOH)_4/TiO_2$ shown in

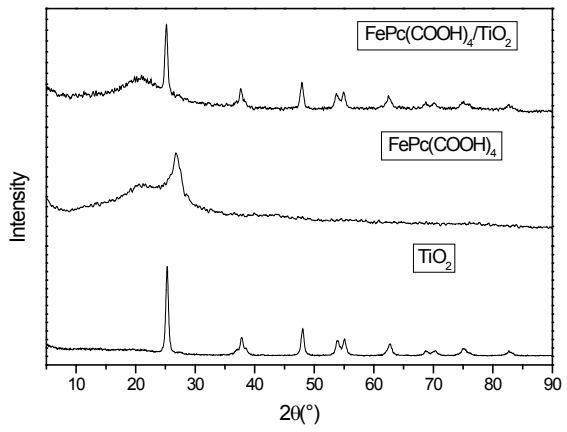

Figure 1: XRD patterns of TiO_2, $FePc(COOH)_4$, and $FePc(COOH)_4/TiO_2$.

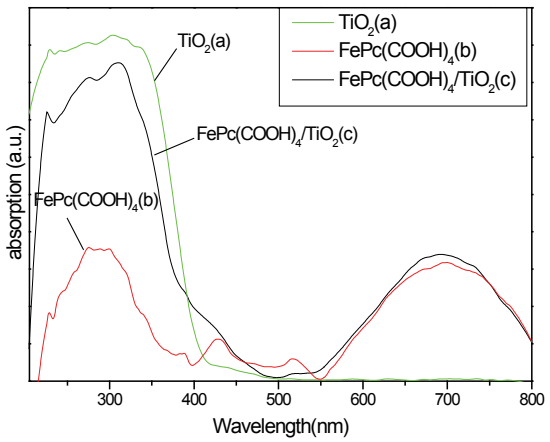

Figure 2: UV-visible diffuse reflectance spectra of TiO_2, $FePc(COOH)_4$, and $FePc(COOH)_4/TiO_2$.

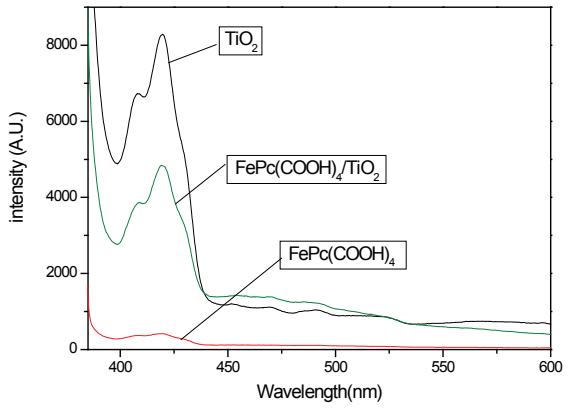

Figure 3: PL spectra of TiO_2, $FePc(COOH)_4$, and $FePc(COOH)_4/TiO_2$.

Figures 4G and H indicate the presence of at least two forms of nitrogen with different chemical properties, i.e., the nitrogen in the 4-pyrrole ring and the 4-azacycle of $FePc(COOH)_4$, respectively.

Photocatalytic degration activity

The photocatalytic degradation of RB was chosen as the model reaction to evaluate the photocatalytic activities of $FePc(COOH)_4/TiO_2$. Pure TiO_2 nanoparticles and $FePc(COOH)_4$ powder were used as reference photocatalysts. The degradation efficiency of the as-prepared samples was defined in terms of the C/C_0 ratio, where C and C_0 represent the remnant and initial concentrations of RB, respectively. As seen in Figure 5, under visible light irradiation, $FePc(COOH)_4/TiO_2$ was completely used in the photodegradation experiment within 100 min and a maximum RB degradation of 96.4% was achieved. In the case of pure TiO_2 and $FePc(COOH)_4$ (reference catalysts), the maximum degradations were only 24.7% and 26.8%, respectively. Hence, RB could be photodegraded efficiently when visible light was used in the presence of $FePc(COOH)_4/TiO_2$.

Figure 6 shows the effect of pH on the oxidative degradation of RB under visible light using $FePc(COOH)_4/TiO_2$ as the photocatalyst. Evidently, the degradation reaction can proceed in a wide pH range (2-12). Adjusting the pH of the initial solution containing RB (6.5 mg/L) with diluted sulfuric acid led to RB conversion rates of 44.8%, 60.2%, and 96.4% at pH=2, 4, and 6, respectively, within 100 min of irradiation. When the degradation reaction was carried out in sodium hydroxide solution, the conversion rates of RB in the same irradiation time were 75.2%, 65.4%, and 36.1% at pH=7, 9, and 10, respectively. Therefore, high rates of RB photodegradation with $FePc(COOH)_4/TiO_2$ can be achieved under approximately neutral pH conditions.

To further examine the catalytic activity of $FePc(COOH)_4/TiO_2$, the degradations of MB, NR, AR, and MG were also investigated. As shown in Figure 7, the various organic dyes were photodegraded by the catalyst within 100 min. When the reaction time was 100 min, the RB, MB, NR, AR, and MG degradation rates were 96.9%, 96.8%, 82.1%, 85.2%, and 81.9%, respectively.

From Table 1 and Figure 8, the curve fitting indicates that the photodegradation reactions follow first-order kinetics. Therefore, $FePc(COOH)_4$-sensitized TiO_2 displays good photocatalytic degradation activity on the various kinds of dyes.

During photocatalysis, TiO_2 acts as the electronic medium and $FePc(COOH)_4$ serves as the sensitizer. When irradiated with light of wavelength >400 nm, the phthalocyanine on the TiO_2 surface is excited and generates $^1O_2$ through energy transfer [32] (as shown in Figure 9). The excited state charges are transferred from the excited state of phthalocyanine in $FePc(COOH)_4$ to the TiO_2 conduction band by electron transfer, resulting in the continuous accumulation of the dye radical cation ($dye^{\cdot+}$) and electrons in the TiO_2 conduction band (e_{cb}^-). In addition, the oxygen molecules and singlet molecular oxygen ($^1O_2$) dissolved in the solution react with the conduction band electrons (e_{cb}^-) to form the superoxide anion radical ($O_2^{\cdot-}$), which is then protonated to generate peroxide radicals (HOO·), which on further reaction generates the strongly oxidizing hydroxyl radicals (OH·) capable of decomposing organic dyes. Phthalocyanine is a solid-state p-type semiconductor with a band gap of about 2.0 eV [33-36]. Since the redox potential of the $dye^{\cdot+}$ radical is 1.2 eV (vs. normal hydrogen electrode, NHE) [23,37], it can oxidize suitable substrates (R) and reduce dyes. Furthermore, TiO_2 can aggregate the excited electrons from the surface of $FePc(COOH)_4$, which are then transferred to TiO_2. These electrons can promote the generation of active oxygen species. In addition to these active oxygen species, the byproduct radical cation $FePc(COOH)_4^{\cdot+}$ can react with the substrate (R) to promote its degradation.

Conclusions

Our studies confirmed that $FePc(COOH)_4/TiO_2$ exhibits good photocatalytic degradation effect on organic dyes, such as MB, RB, NR, AR, and MG. The dye degradation kinetics further demonstrated that the dye solutions could effectively be degraded within 100 min. The photocatalytic degradation followed first-order kinetics. Generally, the industrial wastewater generated from papermaking and textile industries contains a mixture of various complex dyes instead of just a single dye. $FePc(COOH)_4/TiO_2$, which extends the optical absorption range of TiO_2 from the UV region to the visible light region, can be effectively used to degrade such industrial wastes with sunlight, enabling environmentally sustainable waste processing practices.

Dye	Kinetics equation	k/min	R^2	$T_{1/2}$/min
MB	Y=–0.68656–0.02799x	0.02799	0.9915	24.76
NR	Y=0.75606–0.02526x	0.02526	0.9998	27.44
MG	Y=–0.35401–0.01289x	0.01289	0.9942	53.77
AR	Y=–0.3396–0.01321x	0.01321	0.9959	52.47
RB	Y=0.00346–0.03342x	0.03342	0.9916	20.74

Table 1: Kinetics parameters of the degradation of various dyes.

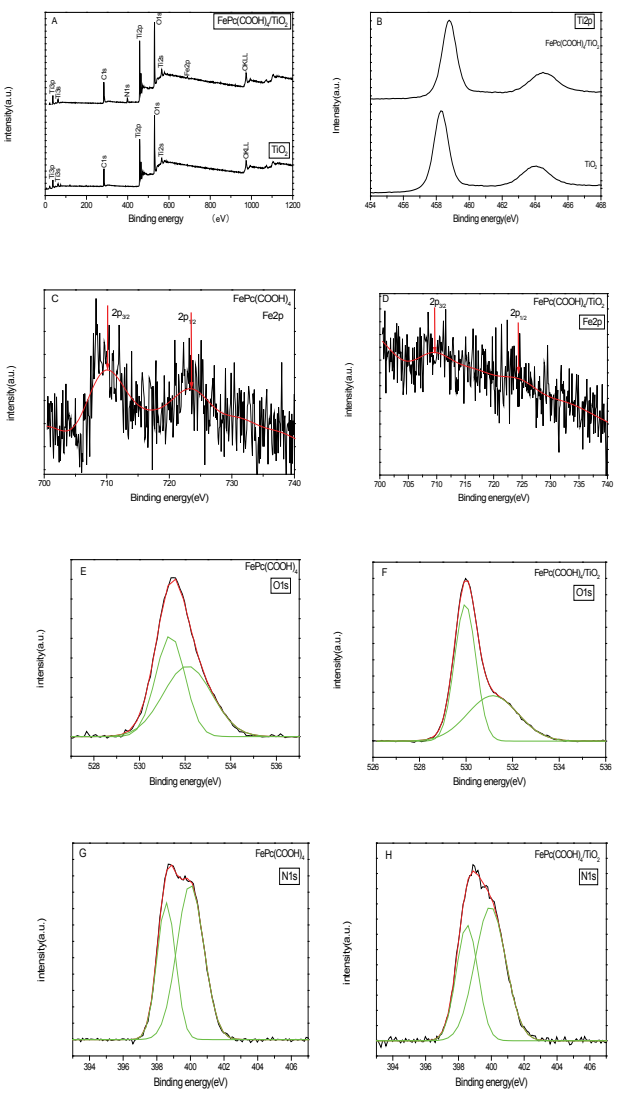

Figure 4: (A) Full scan XPS profiles of $FePc(COOH)_4/TiO_2$ and TiO_2. (B) Ti 2p XPS profiles of $FePc(COOH)_4/TiO_2$ and TiO_2. Fe 2p XPS profiles of (C) $FePc(COOH)_4$ and (D) $FePc(COOH)_4/TiO_2$. O 1s XPS profiles of (E) $FePc(COOH)_4$ and (F) $FePc(COOH)_4/TiO_2$. N 1s XPS profiles of (G) $FePc(COOH)_4$ and (H) $FePc(COOH)_4/TiO_2$.

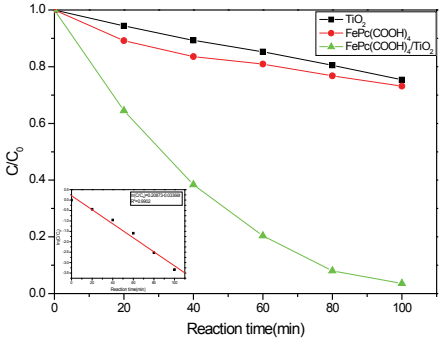

Figure 5: Photodegradation rate of RB in the presence of TiO_2, $FePc(COOH)_4$ and $FePc(COOH)_4/TiO_2$ under visible light irradiation at different periods of time (the initial concentration of RB C_0=6.5 mg/L).

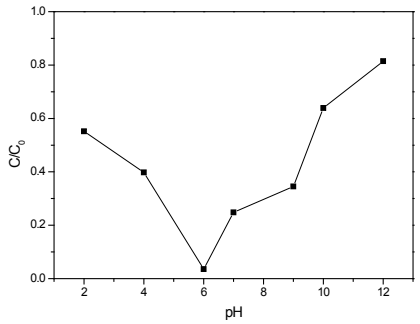

Figure 6: Effect of pH on the photodegradation of RB (6.5 mg/L) in 100 min by visible light irradiation in the presence of $FePc(COOH)_4/TiO_2$.

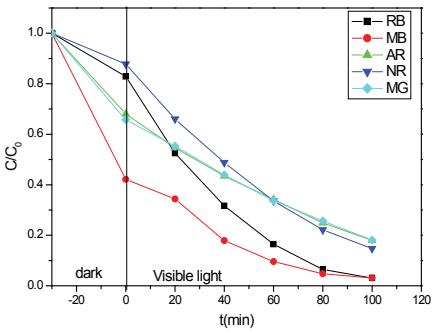

Figure 7: Photodegradation rates of various dyes by $FePc(COOH)_4/TiO_2$.

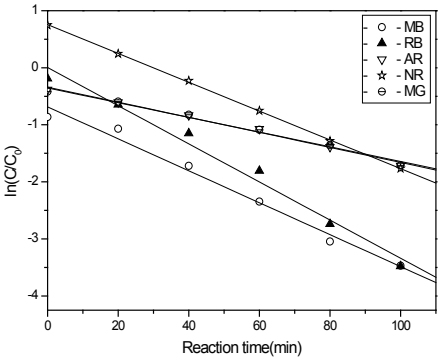

Figure 8: Photodegradation kinetics of the dyes by $FePc(COOH)_4/TiO_2$.

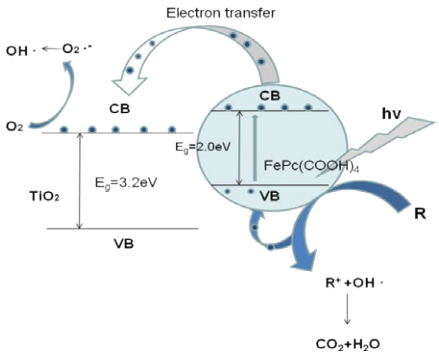

Figure 9: Postulated mechanism for the visible light-induced photodegradation of an organic pollutant (R) by $FePc(COOH)_4/TiO_2$.

Acknowledgements

We gratefully acknowledge financial support from the National Natural Science Foundation of China (Grants No. 21273202 and 21473162). Y. Zhao is grateful to the Project Grants 521 Talents Cultivation of the Zhejiang Sci-Tech University. This work is also supported by the Zhejiang Provincial Top Key Academic Discipline of Chemical Engineering and Technology.

References

1. Litter MI (1999) Heterogeneous photocatalysis: Transition metal ions in photocatalytic systems. Appl Catal B 23: 89-114.
2. Fujishima A, Rao T, Tryk DA (2000) Titanium dioxide photocatalysis. J Photochem Photobiol C 1: 1-21.
3. Andersson M, Osterlund L, Ljungstrm S, Palmqvist A (2002) Preparation of Nanosize Anatase and Rutile TiO_2 by Hydrothermal Treatment of Microemulsions and Their Activity for Photocatalytic Wet Oxidation of Phenol. J Phys Chem B 41: 10674-10679.
4. Anpo M, Takeuchi M (2003) The design and development of highly reactive titanium oxide photocatalysts operating under visible light irradiation. J Catal 12: 505-516.
5. Yin S, Aita Y, Komatsu M, Wang J, Tang Q, et al. (2005) Synthesis of excellent visible-light responsive TiO_2 - xNy photocatalyst by a homogeneous precipitation-solvothermal process. J Mater Chem 6: 674-682.
6. Zhu J, Zheng W, He B, Zhang J. Anpo M (2004) Characterization of Fe–TiO_2 photocatalysts synthesized by hydrothermal method and their photocatalytic reactivity for photodegradation of XRG dye diluted in water. J Mol Catal A 1: 35-43.
7. Tada H, Teranishi K, Inubushi Y, Ito S (1998) TiO_2 photocatalytic reduction of bis(2-dipyridyl)disulfide to 2-mercaptopyridine by H2O: incorporation effect of nanometer-sized Ag particles. Chem Commun 21: 2345-2346.
8. Tada H, Suzuki F, Yoneda S, Ito S (2001) The effect of nanometre-sized Au particle loading on TiO2 photocatalysed reduction of bis(2-dipyridyl)disulfide to 2-mercaptopyridine by H_2O. J Chem Phys 7: 1376-1382.
9. Bae E, Choi W, Park J, Shin H, Kim S, et al. (2004) Effects of Surface Anchoring Groups (Carboxylate vs Phosphonate) in Ruthenium-Complex-Sensitized TiO_2 on Visible Light Reactivity in Aqueous Suspensions. J Phys Chem B 108: 14093-14101.
10. Hagfeldt A, Graetel M (1995) Light-Induced Redox Reactions in Nanocrystalline Systems. Chem Rev 95: 49-68.
11. Fessenden RW, Kamat PV (1995) Rate Constants for Charge Injection from Excited Sensitizer into SnO2, ZnO, and TiO_2 Semiconductor Nanocrystallites. J Phys Chem 34: 12902-12906.
12. Stipkala JM, Heimer TA, Kelly CA, Livi KJT, Meyer G (1997) Light-Induced Charge Separation at Sensitized Sol-Gel Processed Semiconductors. J Chem Mater 11: 2341-2353.
13. Chauke V, Nyokong T (2008) Photocatalytic oxidation of 1-hexene using GaPc and InPc octasubstituted derivatives. J Mol Catal A: Chem 289: 9-13.
14. Sehlotho N, Nyokong T (2004) Zinc phthalocyanine photocatalyzed oxidation of cyclohexene. J Mol Catal A: Chem 219: 201-207.
15. Rudolf S, Gabriela D, Krzysztof S, Giuseppe M, Iolanda P (2011) Photocatalytic activity of nano and microcrystalline TiO2 hybrid systems involving phthalocyanine or porphyrin sensitizers. J Photochemical and Photobiological Sciences 10: 361-366.
16. Fa W, Zan L, Gong C, Zhong J, Deng K (2008) Solid-phase photocatalytic degradation of polystyrene with TiO_2 modified by iron (II) phthalocyanine. J Appl Catal B 79: 216-223.
17. Iliev V, Mihaylova A, Bilyarska L (2002) Photooxidation of phenols in aqueous solution, catalyzed by mononuclear and polynuclear metal phthalocyanine complexes. J Mol Catal A 184: 121-130.
18. Giuseppe M, Elisa G, Leonardo P, Gabriela D, Rudolf S (2007) Photocatalytic Degradation of 4-Nitrophenol in Aqueous Suspension by Using Polycrystalline TiO2 Impregnated with Lanthanide Double-Decker Phthalocyanine Complexes. J Phys Chem C 111: 6581-6588.
19. Ranjit KT, Willner I (1998) Iron(III) Phthalocyanine-Modified Titanium Dioxide: A Novel Photocatalyst for the Enhanced Photodegradation of Organic Pollutants. J Phys Chem B 102: 9397-9403.
20. Tao X, Ma W, Zhang T, Zhao J (2002) A novel approach for the oxidative degradation of organic pollutants in aqueous solutions mediated by iron tetrasulfophthalocyanine under visible light radiation. Chemistry 8: 1321-1326.
21. Sun Q, Xu Y (2009) Sensitization of TiO2 with Aluminum Phthalocyanine: Factors Influencing the Efficiency for Chlorophenol Degradation in Water under Visible Light. J Phys Chem C 113: 12387-12394.
22. Shinohara H, Tsaryova O, Schnurpfeil G, Wohrle D (2006) Differently substituted phthalocyanines: Comparison of calculated energy levels, singlet oxygen quantum yields, photo-oxidative stabilities, photocatalytic and catalytic activities. J Photochem Photobiol A 184: 50-57.
23. Hodak J, Quinteros C, Litter MI, Roman ESJ (1996) Sensitization of TiO_2 with phthalocyanines. Part 1.-Photo-oxidations using hydroxoaluminium tricarboxymonoamidephthalocyanine adsorbed on TiO_2. Chem Soc Faraday Trans 92: 5081-5088.
24. Zhang XF, Lin Y, Guo W, Zhu J (2014) Spectroscopic insights on imidazole substituted phthalocyanine photosensitizers: fluorescence properties, triplet state and singlet oxygen generation. Spectrochim Acta A Mol Biomol Spectrosc 133: 752-758.
25. Ghani F, Kristen J, Riegler H (2012) Solubility properties of unsubstituted metal phthalocyanines in different types of solvents. J Chem Eng Data 57: 439-449.
26. Sharman W (2005) A new procedure for the synthesis of water-soluble tri-cationic and anionic phthalocyanines. J Porphyr Phthalocyanines 9: 651.
27. Achar BN, Lokesh KS (2004) Studies on polymorphic modifications of copper phthalocyanine. J Solid State Chem 177: 1987-1993.
28. Mani V, Devasenathipathy R, Chen S, Gu J, Huang S (2015) Synthesis and characterization of graphene-cobalt phthalocyanines and graphene-iron phthalocyanine composites and their enzymatic fuel cell application. Renew Energy 74: 867-874.
29. Deng L, Wang S, Liu D, Zhu B, Huang W, et al. (2009) Synthesis, Characterization of Fe-doped TiO2 Nanotubes with High Photocatalytic Activity. Catal Lett 129: 513-518.
30. Lin L, Huang X, Wang L, Tang A (2012) Synthesis, characterization and the electrocatalytic application of prussian blue/titanate nanotubes nanocomposite. Solid State Sci 12: 1764-1769.
31. Campbell WM, Burrell AK, Officer DL, Jolley KW (2004) Porphyrins as light harvesters in the dye-sensitised TiO_2 solar cell. Coord Chem Rev 248: 1363-1379.
32. Schlettwein D, Kaneko M, Yamada A, Weohrle D, Jaeger NI (1991) Light-induced dioxygen reduction at thin film electrodes of various porphyrins. J Phys Chem 95: 1748-1755.
33. Loutfy RO, Sharp JH (1979) Photovoltaic properties of metal-free phthalocyanines. I. Al/H_2Pc Schottky barrier solar cells. J Chem Phys 71: 1211.
34. Tang CW (1986) Two-layer organic photovoltaic cell. Appl Phys Lett 48: 183.
35. Popovic ZD (1984) A study of carrier generation in β-metal-free phthalocyanine. Chem Phys 86: 311-321.
36. Iliev V (2002) Phthalocyanine-modified titania-catalyst for photooxidation of phenols by irradiation with visible light. J Photochem Photobiol Chem 151: 195-199.
37. Darwent JR, Douglas P, Harriman A, Porter G, Richoux MC (1982) Metal phthalocyanines and porphyrins as photosensitizers for reduction of water to hydrogen. Coord Chem Rev 44: 83-126.